Structural Engineering and Mechanics, *Vol. 55, No. 1 (2015) 93-109*
DOI: http://dx.doi.org/10.12989/sem.2015.55.1.093

Numerical analysis of crack propagation in cement PMMA: application of SED approach

Benouis Ali*[1], Boulenouar Abdelkader[2], Benseddiq Noureddine[3] and Serier Boualem[1]

[1]*Mechanics and Physics of Materials Laboratory, Djillali Liabes University of Sidi Bel-Abbes, BP89 cité Larbi Ben M'hidi, Sidi Bel-Abbes, Algeria*
[2]*Materials and Reactive Systems Laboratory, Mechanical Engineering Department, University of Sidi-Bel-Abbes, BP. 89, City Larbi Ben Mhidi, Sidi Bel Abbes 22000, Algeria*
[3]*Mechanics Laboratory of Lille, CNRS UMR 8107, Ecole Polytech'Lille, University of Lille1, 59655 Villeneuve d'Ascq, France*

(Received March 1, 2015, Revised March 16, 2015, Accepted May 18, 2015)

Abstract. Finite element analysis (FEA) combined with the concepts of linear elastic fracture mechanics (LEFM) provides a practical and convenient means to study the fracture and crack growth of materials. In this paper, a numerical modeling of crack propagation in the cement mantle of the reconstructed acetabulum is presented. This work is based on the implementation of the displacement extrapolation method (DEM) and the strain energy density (SED) theory in a finite element code. At each crack increment length, the kinking angle is evaluated as a function of stress intensity factors (SIFs). In this paper, we analyzed the mechanical behavior of cracks initiated in the cement mantle by evaluating the SIFs. The effect of the defect on the crack propagation path was highlighted.

Keywords: strain energy density; mixed mode; crack propagation; orthopedic cement

1. Introduction

In the clinical loosening of implants in total hip replacement surgery, fracture of the cement mantle is the main indicated reason (Sanjukta 2008). Cracks initiate from micro-voids in cement and propagate due to the cyclic loading of the human body weight during the walking gate cycles (Pérez *et al.* 2006). Crack growth analysis is important to improve the total hip life span. In literature; there has been a little amount of researches carried out in to the crack's growth path in the orthopedic cement, there has been some studies dealing with the fatigue life of orthopedic cement, but not following the crack's growth path (Jonathan *et al.* 2007, Colombi 2002, Lennon *et al.* 2003, Murphy *et al.* 2001). Byeongsoo *et al.* (2008) analyzed the fracture parameters (K_I, K_{II} and K_{eff}) in a cross section of the femur part of the total hip joint. Benbarek *et al.* (2013) used the finite element method to analyze the propagation's path of the crack in the orthopedic cement of the total hip replacement. Results show that the crack propagation's path can be influenced by human body posture. Hambli (2014) investigated the FE model coupled to quasi-brittle damage

*Corresponding author, Ph.D., E-mail: alimoh1980@yahoo.fr

http://www.techno-press.org/?journal=sem&subpage=8 ISSN: 1225-4568 (Print), 1598-6217 (Online)

law to describe the multiple cracks initiation and to predict the fracture pattern of human proximal femur under quasi-static load. Baofeng *et al.* (2014) examined the effect of overlay on the crack propagation in old cement concrete pavement with an embedded crack and with an asphalt overlay. Benouis *et al.* (2015) investigated the 3D FE method to analyse the distribution of equivalents stress of Von Mises around a cavity located in the bone cement polymethylmethacrylate (PMMA). Results show that the micro-porosity located in the proximal and distal zone of the prosthesis is subject to higher stress field.

In linear elastic fracture mechanics, the various fracture criteria for cracks subjected to mixed mode loading have been introduced for the determination of the propagation direction and the critical stress such as maximum tangential stress criterion (Erdogan *et al.* 1963, Chang 1981, Maiti *et al.* 1983), maximum principal tangential stress criterion (Wu 1974, Chang 1981), maximum strain criterion (Wu 1974 and Chang 1981), and strain energy density criterion (Sih *et al.* 1974, Sih 1974, Kipp *et al.* 1975, Sih *et al.* 1973, Jayatilaka *et al.* 1977, Theocaris 1984). All these criteria are almost postulated that crack initiation will occur at the crack tip and propagate towards the radial direction.

The strain energy density approach has been found as a powerful tool to assess the static and fatigue behavior of notched and unnotched components in structural engineering (Berto *et al.* 2009, Berto *et al.* 2012, Berto and Lazzarin 2014, Lazzarin *et al.* 2013). Different SED-based approaches were formulated by many researchers. (Labeas *et al*. 2006, Zuo *et al.* 2002, Nobile *et al.* 2004, Balasubramanian *et al.* 2000, Ayatollahi *et al.* 2012, Spyropoulos *et al.* 2003).

The aim of this paper is to present a numerical modeling of crack propagation trajectory in cement of reconstructed acetabulum. Using the Ansys Parametric Design Language (APDL) (ANSYS Inc. 2009**)**, the direction crack is evaluated as a function of the displacement extrapolation technique and the strain energy density theory. The finite element method is used to carry out this objective. The effect of the inclusions and cavities on the crack propagation in cement orthopedic was highlighted.

2. Strain energy density theory and SIFs

Sih *et al.* (1974) has postulated the critical value of the local strain energy as a criterion of crack instability. The minimum of strain energy density (SED) around the crack-tip determines the direction of crack propagation. The angle of crack propagation θ can be determined by solving the following equations (Balasubramanian *et al.* 2000)

$$\frac{\partial S}{\partial \theta}=0 \qquad \text{and} \qquad \frac{\partial^2 S}{\partial \theta^2}>0 \tag{1}$$

with

$$S=\frac{dW}{dV}r \tag{2}$$

Where r is its distance from the crack-tip and S is the strain energy density factor.

For the case of mixed modes I and II loadings, the strain energy density factor S was given by Sih as follows

$$S=\frac{1}{\pi}(a_{11}K_I^2+2a_{12}K_1K_{II}+a_{22}K_{II}^2) \tag{3}$$

The coefficients a_{ij} (i,j=1, 2) are determined as

$$a_{11} = \frac{1}{16\mu\pi}\left[(\kappa - \cos\theta)(1+\cos\theta)\right]$$
$$a_{22} = \frac{1}{16\mu\pi}\left[(\kappa+1)(1-\cos\theta) + (1+\cos\theta)(3\cos\theta - 1)\right] \quad (4)$$
$$a_{12} = \frac{1}{16\mu\pi}\left[\sin\theta\,(2\cos\theta - \kappa + 1)\right]$$

where μ is the shear modulus, such that $E=2\mu(1+\nu)$ with E being the Young's modulus, and $k=3-4\nu$ for plane strain and $k=(3-\nu)/(1+\nu)$ for plane stress. dw/dV is elastic energy per unit volume V.

In this paper, the displacement extrapolation method is used to calculate the stress intensity factors K_I and K_{II} as follows (Souiyah *et al.* 2008, Alshoaibi *et al.* 2006, Alshoaibi *et al.* 2007)

$$K_I = \frac{E}{3(1+\nu)(1+k)}\sqrt{\frac{2\pi}{L}}\,[4(v_b - v_d) - \frac{(v_c - v_e)}{2}], \quad (5a)$$

$$K_{II} = \frac{E}{3(1+\nu)(1+k)}\sqrt{\frac{2\pi}{L}}\,(4(u_b - u_d) - \frac{(u_c - u_e)}{2}), \quad (5b)$$

where:

L is the length of the element side connected to the crack-tip.

u_i and v_i (i=b, c, d and e) are the nodal displacements at nodes b, c, d and e in the x and y directions, respectively (see Fig. 1).

In order to obtain a better approximation of the field near crack-tip, special quarter point finite elements proposed by Barsoum (1974) are used where the mid-side node of the element in the crack-tip is moved to 1/4 of the length of the element, as shown in Fig. 1.

2. Geometric and Material's definition

The model was generated from a roentgenogram of 4mm slice normal to the acetabulum through the pubic and ilium. The inner diameter of the UHMWPE cup is 54 mm and the cement

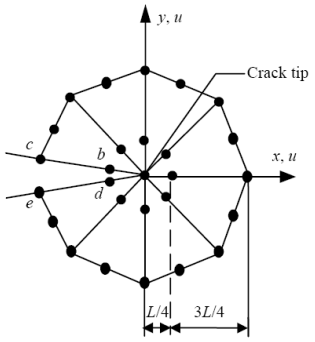

Fig. 1 Special elements used for displacement extrapolation technique

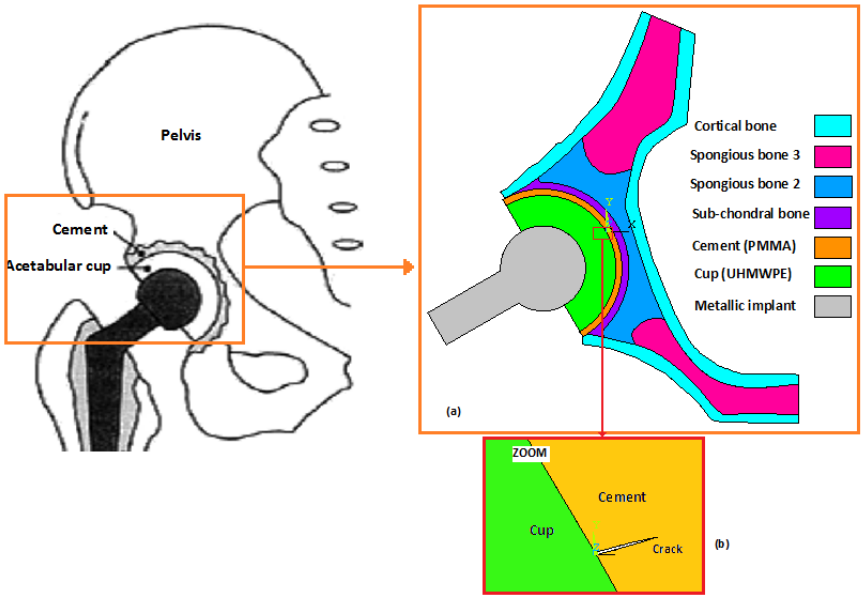

Fig. 2 (a) Geometrical model, (b) Initial crack emanating from interface cup/cement

Table 1 Mechanical properties of materials used in the study (Kayabasi *et al.* 2006)

Materials	Young modulus E (MPa)	Poisson ratio (v)
Cortical bone	17000	0.30
Sub-chondral bone	2000	0.30
Spongious bone 2	70	0.20
Spongious bone 3	2	0.20
Cup (UHMWPE)	690	0.35
Cement (PMMA)	2300	0.30
Metallic implant	210000	0.30

thickness was taken as 2 mm (Benbarek *et al.* 2009, Benbarek *et al.* 2007, Tong *et al.*). Fig. 2(a) presents the geometrical model used in this study. The initial crack of length of a=50 μm emanating from the interface cup/cement is supposed to exist in the cement layer (Fig. 2(b)).

The model was divided into seven regions (Fig. 2(a)) of different elastic constants with isotropic material properties assumed in each region. The femoral head was modelled as a circularize surface that was mated with congruent spherical acetabular socket. The mechanical properties of cement, cup and all subregions of the acetabulum bone are given in Table 1.

3. Loading conditions

In this section, the force F=2400 N is applied to the centre of the femoral head (Fig. 3). These conditions of loading are considered as the extreme case of an effort which the prosthesis can support. It is the force which man can exert on only one support at time of rise of staircase (Leroy 1991). The model used in this study allows us to reproduce all the phases of each movement by

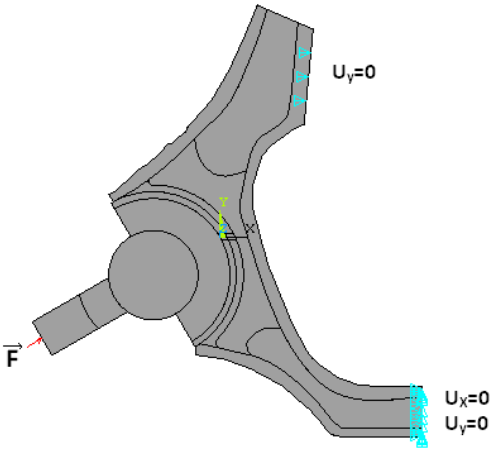

Fig. 3 Boundary conditions

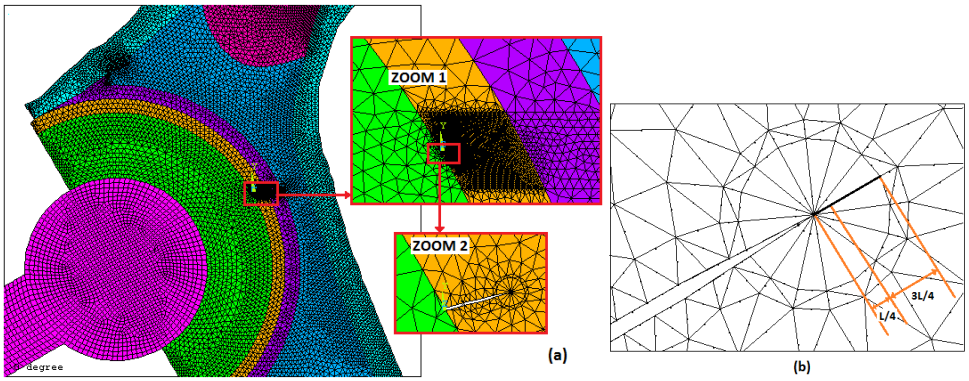

Fig. 4 (a) Mesh model and (b) Special elements used for displacement extrapolation method

changing the direction of the applied force (Dalstra *et al.* 1995). The loading cases analysed in this study correspond to 0° of the metallic implant position. It is the cases when the femoral head is in contact with one extremity of the cup. A great area of the left part of cement is in tension. Fig. 3 shows boundary conditions acting on the model. The boundary conditions imposed on the geometrical model are taken from the references (Benbarek *et al.* 2013). In Fig. 3, u_x and u_y indicate the displacements in the x and y directions, respectively.

5. Finite element model

Computational methods such as finite element method are widely accepted in orthopaedic biomechanics as an important tool used to design and analysis the mechanical behaviour of prosthesis (Nocollela *et al.* 2001). Several authors used this method to analyse the mechanical behaviour of hip prosthesis, among them, we can quote: (Colombi 2002, Lennon *et al.* 2003, Harry *et al.* 1991, Sim *et al.* 1995, Weiman *et al.* 1993, Doblaré *et al.* 2002, Oguz *et al.* 2008, Ahmet 2010, Dyrkacz *et al.* 2015).

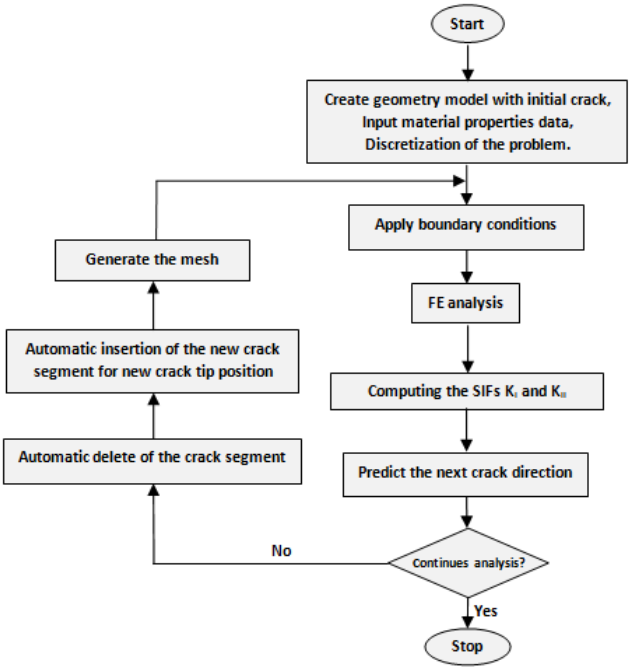

Fig. 5 Flow chart of FEM algorithm of the problem

Contributing to this field, we analysed the behaviour and propagation of cracks in the cement layer, which fix the acetabular cup to the contiguous bon, by calculating the SIFs around the crack tip.

For the mesh generation of the cracked plate, the element type 'PLANE183' of ANSYS code is used. It is a higher order two dimensional, 8-node element having two degrees of freedom at each node (translations in the nodal x and y directions), quadratic displacement behavior and the capability of forming a triangular-shaped element, which is required at the crack tip areas.

A typical FE model is shown in Fig. 4(a). The special quarter point singular elements proposed by (Barsoum 1974), are used for modeling the singular field near the crack tip (Fig. 4(b)). This mesh will serve to calculate the stress intensity factors K_I and K_{II} using the displacement extrapolation method implemented in ANSYS software.

4. Crack growth algorithm

This section presents a finite element analysis for modeling fracture problems in orthopedic cement. Fig. 5 shows the flow-chart of the prepared APDL code based on the combination of the finite element analysis and the strain energy density concept. According to the algorithm, after initial geometrical and physical modeling of the problem, the mesh pattern is generated around crack tip. In order to find new crack tip position at each step of propagation, the displacement extrapolation technique and the strain energy Sih's theory are employed, to obtain the SIFs and the crack direction. At each increment Δa of crack propagation, the special mesh is generated around crack tip, using the quadratic six-node triangular element. It is noted that, the same numeration of

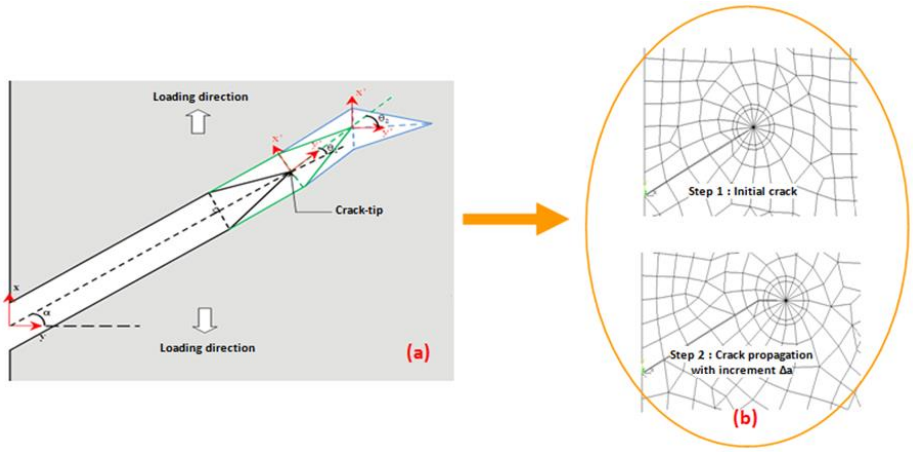

Fig. 6 (a) Crack propagation mechanism proposed in this study, (b) FE modeling for crack propagation

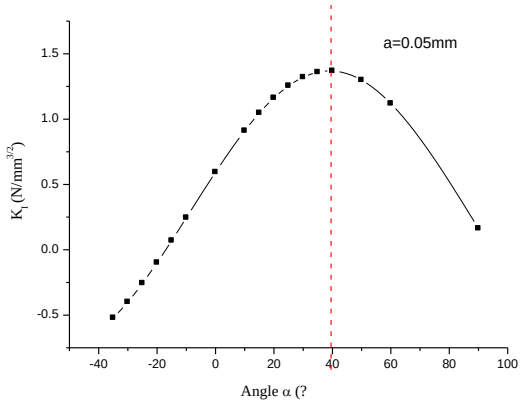

Fig. 7 Variation of K_I vs. inclination angles α (a=0.05 mm)

the nodes around the crack tip is taken during the crack propagation to calculate automatically the SIFs K_I and K_{II}, using Eq. (5a) and (5b). The algorithm is repeated until ultimate failure of material or by using another criterion for termination of the simulation process. Fig. 6 illustrates the crack propagation mechanism proposed in this study.

3. Results and discussion

3.1 Evolution of stress intensity factors

In order to simulate the behavior of a crack under mixed mode loading (mode I+II); we considered an example of a crack of length 50 μm in cement layer. This crack is inclined to the horizontal x-axis from −35° to 90° (see Fig. 2(b)).

Figs. 7 and 8 show, respectively, the variation of the SIFs K_I and K_{II} vs. the inclination angles of crack in cement layer.

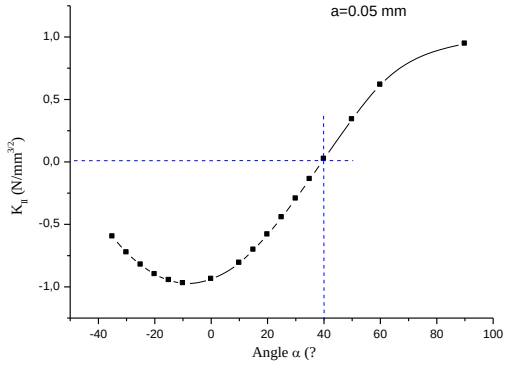

Fig. 8 Variation of K_{II} vs. inclination angles α (a=0.05 mm)

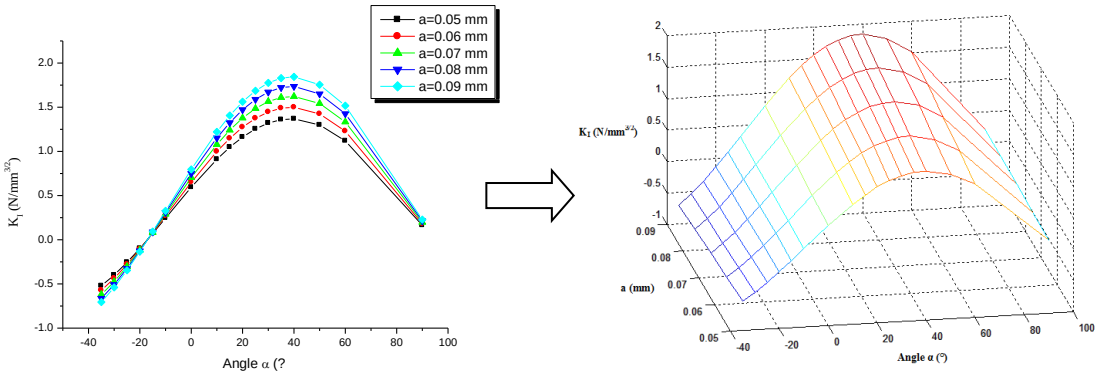

(a) (b)

Fig. 9 Variation of SIF K_I vs. crack size a and angle α: (a) in 2D and (b) in 3D

The results obtained in Fig. 7 show that:

1. The SIF K_I is maximum when the angle α=40°, then it decreases gradually with the increase of the positive angle and tends to a very low value as one approaches the Cup-Cement interface.

2. The factor K_I decreases with the angle α, up to a minimal value corresponds to an angle α=−18° from which factor K_I takes values negative with the decrease of the angle α.

The SIF K_{II} is null when the inclination angle α=40° and increases with this angle (Fig. 8). The factor K_{II} decreases with the angle α up to a minimal value corresponds to an angle α≈−18° from which the curve takes on a downward look with the decrease of angle α.

Through these results, we can conclude that the angle of 40° represents the initial direction of the crack propagation according to the opening mode (mode-I) with: K_I> 0 and K_{II}=0.

For better a study of these parameters, we represented respectively, in Fig. 9(a) and 9(b), the variation of the SIFs K_I and K_{II} vs. the inclination angles α, by variation of initial crack size. We note exactly the same behavior of the SIFs K_I and K_{II} as in the as in the previous case. In addition, we note that:

√ The SIF K_I increases with the crack length and takes values positive for angles in the range between 90° and −18°, some is the inclination angles α, i.e., it does not depend on the direction of initial crack.

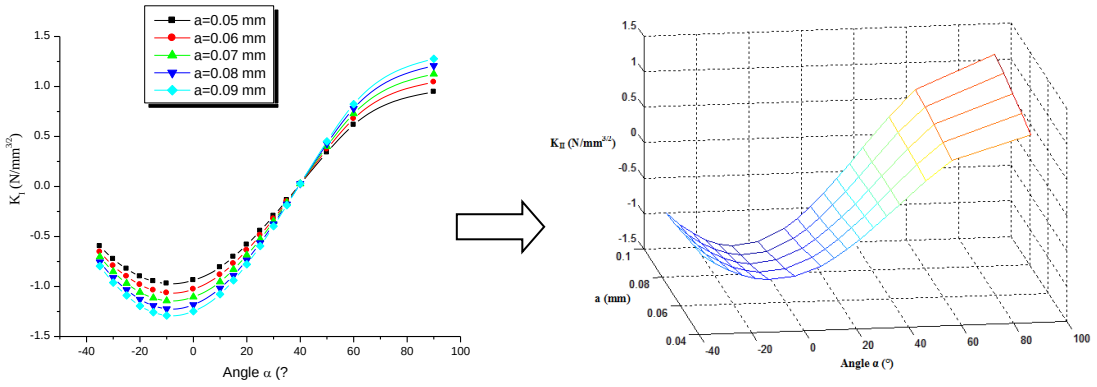

(a) (b)

Fig. 10 Variation of SIF K_{II} vs. crack size a and angle α: (a) in 2D and (b) in 3D

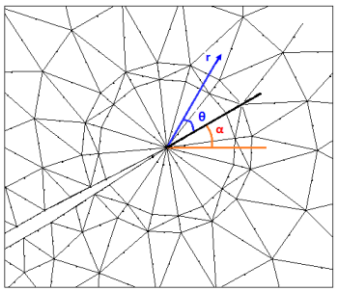

Fig. 11 Description of the parameters r, α and θ

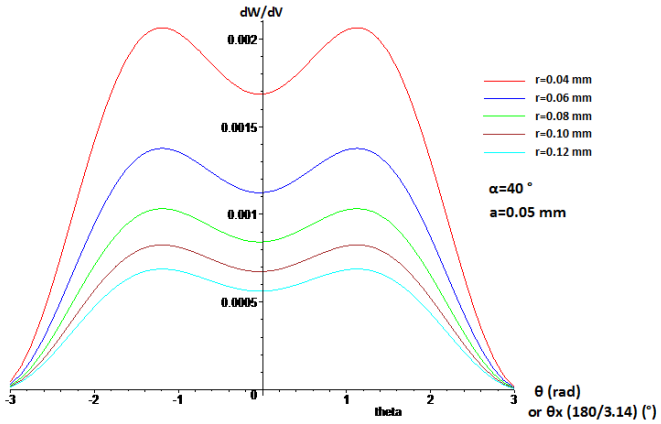

Fig. 12 Variation of (dw/dv) vs. initial angle of propagation

√ For cracks initiated in the range between −35 and −18°, the factor K_I present of the values negative, this can is explained by the existence of the crack in the compression zone.

Fig. 10 show that, in the case of the angles α vary between −35° and 90°, the SIF K_{II} takes positive values and its negative values are evaluated in the opposite case, i.e., it depends on the direction of crack orientation. This behavior is similar with this remark by Boulenouar *et al.*

(2013), in the case of cracked plate under mixed mode loading.

The results obtained show that, whatever the crack length, the angle of 40° represents the initial direction of the crack propagation according to the mode-I.

3.2 Minimal strain energy density criterion

Fig. 11 illustrates the description of the parameters: r, α and θ. Where: r is the distance from the crack-tip, α is the crack inclination angle and θ is the kinking angle.

Using the equations 1, 2 and 3, we represented in Fig. 12, the evolution of the strain energy density SED according to the radius r and of the initial angle of propagation θ. One can notice, that apart from a certain zone around the crack tip, the minimum of the density of deformation energy (dw/dv)min of (dw/dv) is reached for a constant value $\theta=\theta_0$ independently of radius r.

3.3 Crack propagation simulation

In the case of a cracked structure under mixed mode loading, the crack does not propagate in a straight line, and it is necessary to determine the direction of crack trajectory. Many criteria have been proposed to determine the kinking angle of the crack propagation. Once this particular angle, the crack propagates a distance Δa. More this distance is small, and the closer to the exact solution. Most authors prefer set Δa as a user setting, preferably small (Červenka 1994). For our part, to determine whether the criterion used in this study provides a good final crack trajectory, we have performed our numerical calculation with a succession of crack increment length Δa=20 μm.

In this section, we propose to study the propagation path of three cracks, a crack inclined to the horizontal x-axis with α=40° and two other cracks which are symmetries to the first crack (for example, one takes the angles 20° and 60°).

The determination of the SIFs K_I and K_{II}, the possible direction and the path propagation of these cracks are carried out under plane stress conditions with the same boundary conditions. Fig. 13 shows the final crack trajectory for three inclination angles (α=20°, 40° and 60°).

The calculations carried out using SED approach, show that the two crack propagations for α=20° and 60° are symmetries to the propagation trajectory possible of the crack inclined with α=40° (Fig. 14).

In the general case, we can still note that we can have the same trajectory of propagation for other cracks which have a symmetry to the crack inclined with α=40°. Fig. 15 shows the final crack trajectory for three inclination angles (α=30°, 40° and 50°).

In order to determine the effect of a geometry defect on the crack propagation, we chose a circular cavity of radius r=100 μm located in cement layer, at a vertical distance y=0.25 mm from

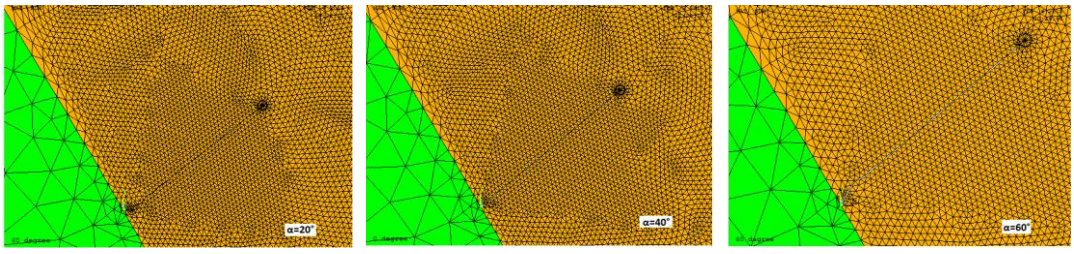

Fig. 13 Crack propagation trajectory (20 steps) with: α=20°, 40° and 60°

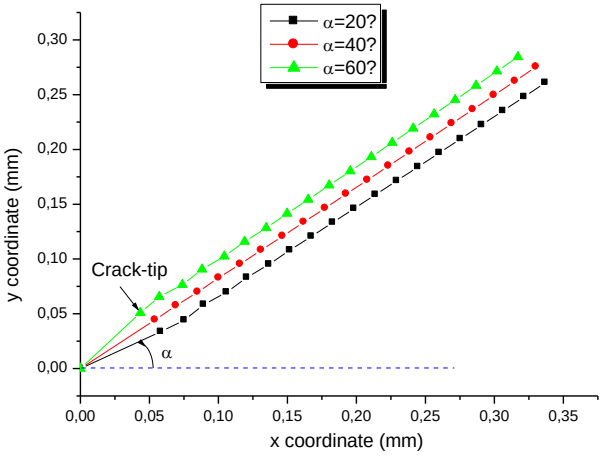

Fig. 14 Crack propagation trajectory with: α=20°, 40° and 60°

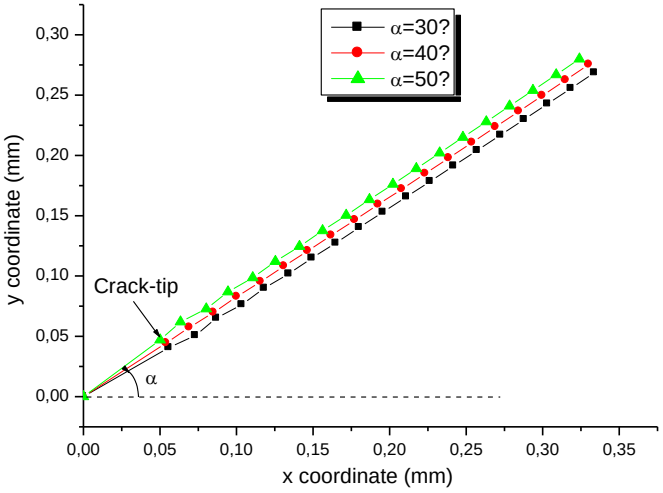

Fig. 15 Crack propagation trajectory with: α=30°, 40° and 50°

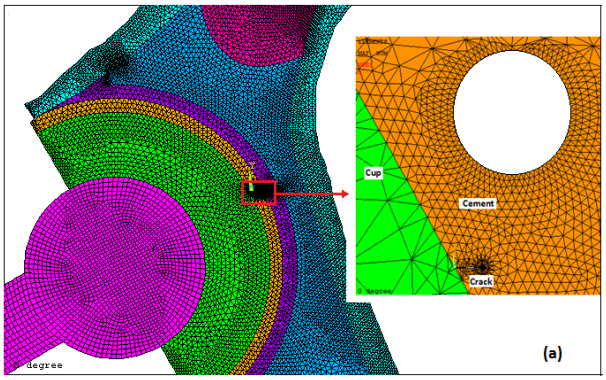

Fig. 16 Typical mesh model near the cavity and the crack

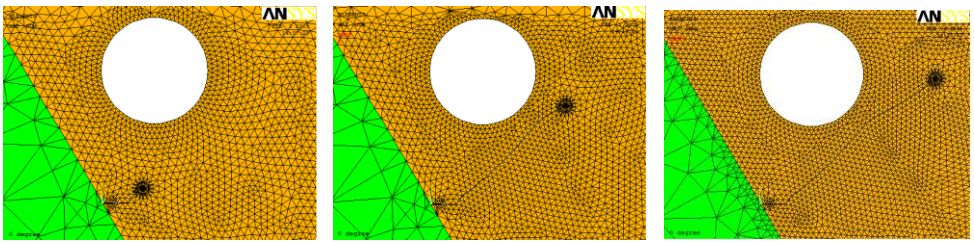

Fig. 17 Three steps of crack propagation (Cavity effect)

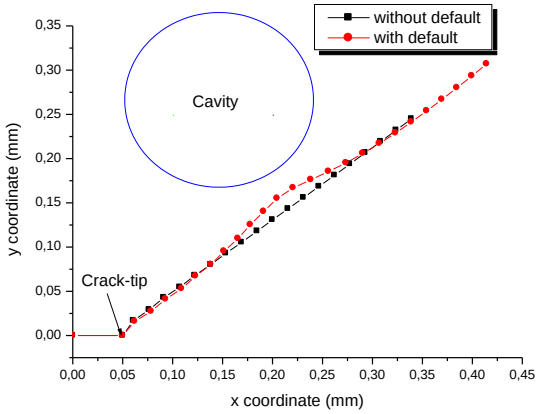

Fig. 18 Cavity effect on the propagation path

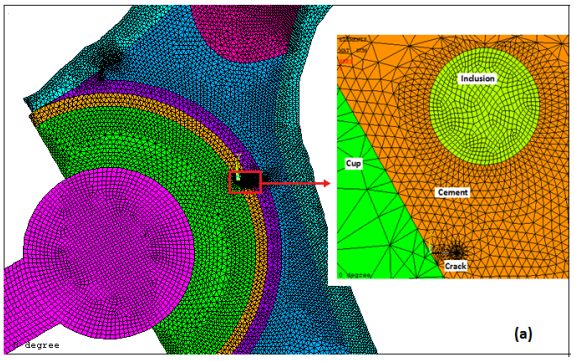

Fig. 19 Typical mesh model near the inclusion and the crack

the crack tip. The geometrical model is meshed by triangular elements and by special quarter point singular elements around the crack-tip (Fig. 16).

Fig. 17 presents three steps of crack propagation path. We find that the crack is moving towards the cavity. This is because the cavity creates a "depression" of stress that will change the maximum principal stress in the cement layer and drew the crack. Once the cavity past, this crack is shifting under mode I loading, and it departs slightly from the cavity (Fig. 19). The comments we get correspond with those obtained by Banbarek *et al.* (2013) for crack growth path in the cement mantle of the reconstructed acetabulum using the maximal circumferential stresses criterion.

In what follows, we propose to study the crack propagation in our model containing an inclusion of radius r=10 μm. Fig. 19 shows the typical mesh model near the inclusion and the crack.

We recall that the mechanical properties of the cement are: Young's modulus E_1=2300 MPa and Poisson's ratio v_1=0, 3 and the inclusion considered is characterized by its Young's modulus E_2 and Poisson's ratio v_2=v_1.

To demonstrate the inclusion effect on the propagation path, we evaluated for three ratios E_2/E_1=1, 0.1 and 10, the SIFs and the kinked direction for each increment Δa to predict then the propagation path. Fig. 18 show respectively the steps of crack trajectory for three ratios E_2/E_1=1, 0.1 and 10. A calculation made by our integrated model shows that:

(a) When the matrix (cement layer) and inclusion have the same mechanical properties (E_2/E_1=1), the crack is propagated in its possible direction as a single homogeneous material (Fig. 20(a)).

(b) In the case of the inclusion less rigid than the matrix (E_2/E_1=0.1), we find a result similar to that which had been obtained for the cracked cement with a cavity (see Fig. 17); this inclusion changes the stress distribution and attracts the crack. Once the inclusion exceeded the crack in its possible direction (Fig. 20(b)).

(c) In the case of the inclusion is more rigid than the cement (E_2/E_1=10), the crack is this time slightly delayed (Fig. 20(c)).

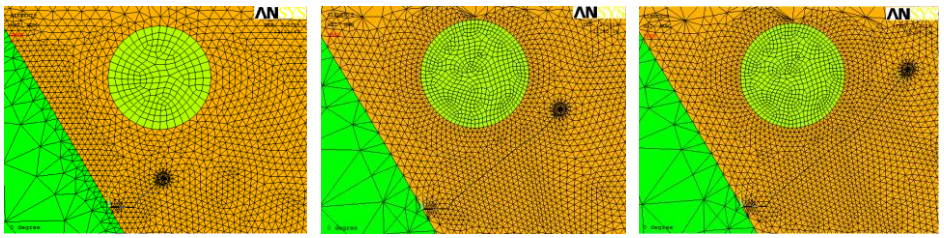

E_2/E_1=1

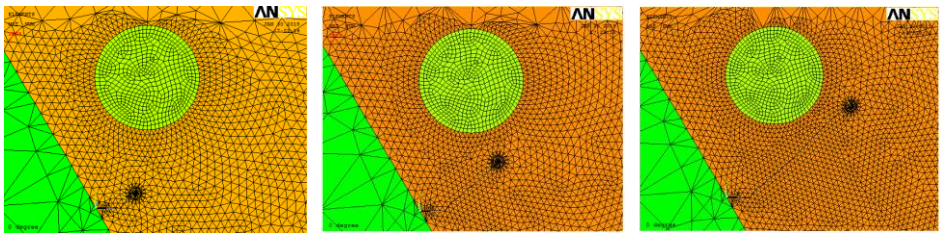

E_2/E_1=0.1

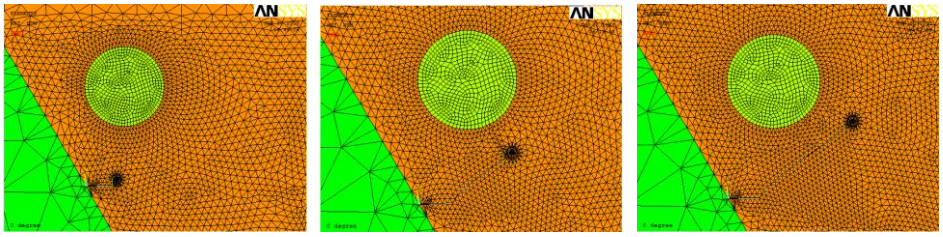

E_2/E_1=10

Fig. 20 Inclusion effect on the propagation path with: (a) E_2/E_1=1, (b) E_2/E_1=0.1, (c) E_2/E_1=10

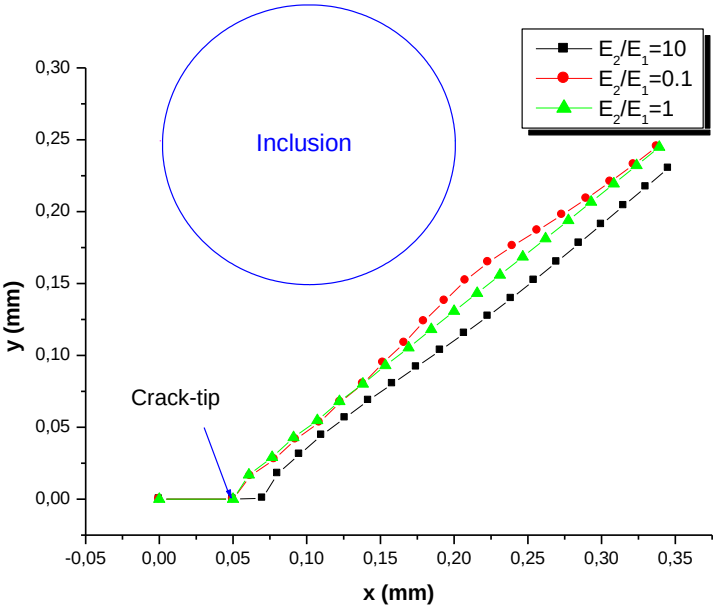

Fig. 22 Inclusion effect on the propagation path

Fig. 22 shows the final crack trajectory for three cases (E_2/E_1=1, 0.1 and 10). The comments we get correspond with those obtained in the case of cracked plates with inclusions (Boulenouar *et al.* 2014, Boulenouar *et al.* 2013, Bouchard *et al.* 2003).

4. Conclusions

In this study, the quarter-point singular elements proposed by Barsoum are used to consider the singularity of stress and deformations fields at crack tip in cement of reconstructed acetabulum.

The displacement extrapolation technique was used to determine the SIFs to predict then the final crack trajectory by evaluation, for each propagation step, the kinked angle using the strain energy density approach.

Numerical calculations made by FEM have shown that the integrated model can correctly describe the stress and deformation field near the crack tip by evaluating the SIFs, and the results are very acceptable on the crack propagation in Biomechanics fracture problems.

The good trajectory of crack under mixed mode conditions is dependent on the crack increment length; over this distance is small, and the closer to the exact solution. The angle of 40° represents the initial direction of the crack propagation according to the opening mode (mode-I) with: $K_I > 0$, $K_{II}=0$

The implementation of 2D crack propagation process in FE code can account for the influence of inclusions on the path of crack propagation. This feature can be very interesting for propagation in multilayered or in composite parts.

References

Ali, B., Boualem, S. and Smail, B. (2015), "Influence of porosity on the behavior of cement orthopaedic of total hip prosthesis", *Adv. Biomech. Appl.*, **2**(1), 1-10.

Alshoaibi, A.M. and Ariffin, A.K. (2006), "Finite element simulation of stress intensity factors in elastic-plastic crack growth". *J. Zhejiang Univ. Sci. A.*, **7**, 1336-1342.

Alshoaibi, A.M., Hadi, M.S.A. and Ariffin, A.K. (2007), "An adaptive finite element procedure for crack propagation analysis", *J. Zhejiang Univ. Sci. A.*, **2**, 228-236.

ANSYS Inc. (2009), Programmer's Manual for Mechnical APDL, Release 12.1.

Ayatollahi, M.R. and Karo, S. (2012), "Mode I fracture initiation in limestone by strain energy density criterion", *Theor. Appl. Fract. Mech*., **57**, 14-18.

Balasubramanian, V. and Guha, B. (2000), "Fatigue life prediction of welded cruciform joints using strain energy density factor approach", *Theor. Appl. Fract. Mech*., **34**, 85-92.

Balasubramanian, V. and Guha, B. (2000), "Fatigue life prediction of welded cruciform joints using strain", *Theor. Appl. Fract. Mech*., **31**, 85-92

Barsoum, R.S. (1974), "On the use of isoparametric finite element in linear fracture mechanics", *Int. J. Numer. Meth. Eng.*, **10**, 25-37.

Benbarek, S., Bachir Bouiadjra, B., Achour, T., Belhouari, M. and Serier, B. (2007), "Finite element analysis of the behaviour of crack emanating from microvoid in cement of reconstructed acétabulum", *Mater. Sci. Eng. A*, **457**, 385-391.

Benbarek, S., Bachir Bouiadjra, B., Mankour, A., Acour, T. and Serier, B., (2009), "Analysis of fracture behaviour of the cement mantle of reconstructed acetabulum", *Comput. Mater. Sci.*, **44**, 1291-1295.

Benbarek, S., Bouiadjra, B.A.B., El Mokhtar, B.M., Achour, T. and Serier, B. (2013), "Numerical analysis of the crack growth path in the cement mantle of the reconstructed acétabulum", *Mater. Sci. Eng. C*, **33**, 543-549.

Berto, F. and Lazzarin, P. (2009), "A review of the volume-based strain energy density approach applied to V-notches and welded structures", *Theor. Appl. Fract. Mech*., **52**, 183-194.

Berto, F., Lazzarin, P. and Marangon, C. (2012), "Brittle fracture of U-notched graphite plates under mixed mode loading", *Mater. Des.*, **41**, 421-432.

Berto, F. and Lazzarin, P. (2014), "Recent developments in brittle and quasi-brittle failure assessment of engineering materials by means of local approaches", *Mater. Sci. Eng. R*, **75**, 1-48.

Bouchard, P.O., Bay, F. and Chastel, Y. (2003), "Numerical modelling of crack propagation: automatic remeshing and comparison of different criteria", *Comput. Meth. Appl. Mech. Eng.*, **192**, 3887-3908.

Boulenouar, A., Benseddiq, N. and Mazari, M. (2013), "Strain energy density prediction of crack propagation for 2D linear elastic materials", *Theor. Appl. Fract. Mech*., **67-68**, 29-37.

Boulenouar, A., Benseddiq, N. and Mazari, M. (2013), "Two-dimensional numerical estimation of stress intensity factors and crack propagation in linear elastic analysis", *Eng. Tech. Appl. Sci. Res.*, **3**, 506-510.

Boulenouar, A., Benseddiq, N., Mazari, M. and Benamara, N., (2014), "FE model for linear elastic mixed mode loading: estimation of SIFs and crack propagation", *J. Theor. Appl. Mech.*, **52** (2), 373-383.

Červenka, J. (1994), "Discrete crack modeling in concrete structures", PhD Thesis of the University of Colorado.

Chang, K.J. (1981), "Further studies of the maximum stress criterion on the angled crack problem". *Eng. Fract. Mech.*, **14**, 125.

Chang, K.J. (1981), "On the maximum strain criterion - a new approach to the angled crack problem", *Eng. Fract. Mech*., **14**, 107-124.

Cilingir, A.C. (2010), "Finite element analysis of the contact mechanics of ceramic-on-ceramic hip resurfacing prostheses", *J. Bio. Eng*., **7**(3), 244-253.

Colombi, P. (2002), "Fatigue analysis of cemented hip prosthesis: damage accumulation scenario and sensitivity analysis", *Int. J. Fatigue*, **24**(7), 739-746.

Dalstra, M. and Huiskes, R. (1995), "Load transfer across the pelvic bone", *J. Biomech*., **28**(6), 715-724.

Deb, S. (2008), *Orthopaedic Bone Cements*, Woodhead Publishing in Materials, First Publishing.
Dooblaré, M. and Garcia, J.M., (2002), "Anisotropic bone remodelling model based on a continuum damage-repair theory", *J. Biomech*., **35**(1), 1-17.
Dyrkacz, R.M.R., Brandt, J.M., Morrison, J., O'Brien, S.T., Ojo, O.A., Turgeon, T.R. and Wyss, U.P. (2015), "Finite element analysis of the head-neck taper interface of modular hip prostheses", *Tribology International*. (in Press)
Erdogan, F. and Sih, G.C. (1963), "On the crack extension in plates under plane loading and transverse shear", *J. Basic Eng.*, **85**, 519-527.
Harigan, T.P. and Harris, W.H. (1991), "A finite element study of the effect of diametral interface gaps on the contact areas and pressures in uncemented cylindrical femoral total hip components", *J. Biomech.*, **24**, 87-91.
Jayatilaka, A.D.S., Jenkins, I. and Prasad, S.V. (1977), "Determination of crack growth in a mixed mode loading system, Analysis and Mechanics", *ICF4*, Waterloo, Canada.
Jeffers, J.R., Browne, M., Lennon, A.B., Prendergast, P.J. and Taylor, M. (2007), "Cement mantle fatigue failure in total hip replacement: experimental and computational testing", *J. Biomech.*, **40**, 1525-1533.
Kim, B.S., Moon, B.Y., Mann, K.A., Kim, H.S. and Boo, K.S. (2008), "Simulated crack propagation in cemented total hip replacements", *Mater. Sci. Eng. A*, **483-484**, 306-308.
Kipp, M.E. and Sih, G.C. (1975), "The strain energy density failure criterion applied to notched elastic solids", *Int. J. Solid. Struct*., **11**, 153-173.
Labeas, G. and Kermanidis, Th. (2006), "Stress multiaxiality factor for crack growth prediction using the strain energy density theory", *Theor. Appl. Fract. Mech*., **45**, 100-107.
Lazzarin, P., Berto, F. and Ayatollahin, M.R. (2013), "Brittle failure of inclined key-hole notches in isostatic graphite under in-plane mixed mode loading", *Fatigue Fract. Eng. Mater. Struct.*, **36**, 942-955.
Lennon, A.B., McCormack, B.A.O. and Prendergast, P.J. (2003), "The relationship between cement fatigue damage and implant surface finish in proximal femoral prostheses", *Med. Eng. Phys.*, **25**, 833-841.
Lennon, A.B. and Pendegast, P.J. (2001), "Evaluation of cement stresses in finite element analyses of cemented orthopaedic implants", *J. Biomech. Eng.*, **123**(6), 623- 628.
Leroy, R. (1991), "Etude et comportement non-uniforme de l'interface entre implant Fémorale et liant polymérique dans le cas de prothèse totale de hanche", Thèse de doctorat, Université de Tours.
Maiti, S.K. and Smith, R.A. (1983), "Comparison of the criteria for mixed mode brittle fracture based on the preinstability stress-strain field", *Int. J. Fracture*, **23**, 281-295.
Murphy, B.P. and Prendergast, P.J. (2001), "The relationship between stress, porosity and nonlinear damage accumulation in acrylic bone cement", *J. Biomed. Mater. Res.*, **59**, 646-654.
Nobile, L., Carloni, C. and Nobile, M. (2004), "Strain energy density prediction of crack initiation and direction in cracked T-beams and pipes", *Theor. Appl. Fract. Mech*., **41**, 137-145.
Nocollela, P.N., Thacker, B.H., Katoozian, H. and Davy, D.T. (2001), *Bioengineerion Conférence*, BED **50**, 427-428.
Kayabasi, O. and Ekici, B. (2008), "Probabilistic design of a newly designed cemented hip prosthesis using finite element method", *Mater. Des.*, **29**(5), 963-971.
Pan, B.F., Gao, Y.Y. and Zhong, Y. (2014), "Theoretical analysis of overlay resisting crack propagation in old cement concrete pavement", *Struct. Eng. Mech.*, **52**(4), 829-841.
Pérez, M.A., Garcia-Aznar, J.M., Doblaré, M., Seral, B. and Seral, F., (2006), "A comparative FEA of the deboning process in different concepts of cemented hip implants", *Medi. Eng. Phys.*, **28**, 525-533.
Ridha, H. (2014), "3D finite element simulation of human proximal femoral fracture under quasi-static load", *Adv. Biomech. Appl.*, **1**(1), 1-14.
Sih, G.C. (1973), "Some basic problems in fracture mechanics and new concepts", *Eng. Fract. Mech*., **5**, 365-377.
Sih, G.C. (1974), "Strain-energy-density factor applied to mixed-mode crack problems", *Int. J. Fract.*, **10**, 305-321.
Sih, G.C. and Macdonald, B. (1974), "Fracture mechanics applied to engineering problems-Strain energy density fracture criterion", *Eng. Fract. Mech*., **6**, 361-386.

Sim, E., Freimuller, W. and Reiter, T.J. (1995), "Finite element analysis of the stress distributions in the proximal end of the femur after stabilization of a pertrochanteric model fracture: a comparison of two implant", *Injury*, **26**, 445-449.

Souiyah, M., Alshoaibi, A.M., Muchtar, A. and Ariffin, A.K. (2008), "Finite element model for linear-elastic mixed mode loading using adaptive mesh strategy", *J. Zhejiang Univ. Sci. A.*, **9**, 32-37.

Spyropoulos, C.P. (2003), "Crack initiation direction from interface of bonded dissimilar media", *Theor. Appl. Fract. Mech.*, **39**, 99-105.

Theocaris, P.S. (1984), "A higher-order approximation for the T-criterion of fracture in biaxial fields", *Eng. Fract. Mech.*, **19**, 975.

Tong, J. and Wong, K.Y. (2005), *Mixed Mode Fracture in Reconstructed Acetabulum, Department of Mechanical and design Engineering, University of Portsmouth*, Anglesea Road, Portsmouth, PO1 3 DJ, UK.

Weinas, H., Huiskes, R., Van ribergen, B., Summer, D.R., Turner, T.M. and Galante, J.O. (1993), "Adaptive bone-remodeling around bonded noncemented THA: a comparison between animal experiments and computer simulatio", *J. Orthopaed. Res.*, **11**, 500-513.

Wu, H.C. (1974), "Dual failure criterion for plane concrete", *J. Eng. Mech. Div.*, ASCE, **100**, 1167-1181.

Zuo, J.Z. Kermanidis, A.T. and Pantelakis, S.G. (2002), "Strain energy density prediction of fatigue crack growth from hole of aging aircraft structures", *Theor. Appl. Fract. Mech.*, **38**, 37-51.

CC